nomenon, the reduction of the folded rotamer population in the LL pseudoequatorial isomer could be a measure of how much the side chains actually interfere with one another, even in this $\beta > 0°$ situation.

On the other hand the LL pseudoequatorial case (Figure 8b) might be thought to have infrequent side chain–side chain contact, and thus be considered the "normal" sterically controlled isomer by virtue of the fact that the phenyl group is not able to come as close to the diketopiperazine ring as it can when the side chains are axially disposed. The high population of fold rotamer in the LD axial isomer would then be due to a special ring–ring interaction.

Given the NMR-determined rotamer populations, it seems that the former explanation is more plausible, because the LL pseudoequatorial isomer of c-(L-NMePhe)$_2$ probably has significant side chain–side chain contact. If the NMR rotamer populations of both side chains are considered to be uncorrelated in $CDCl_3$ and Me_2SO, the two side chains would be nearly in contact approximately 25% of the time. Thus it is likely that the interaction between side chains forces the diketopiperazine ring into $\beta > 0°$ conformation in the first place. This view of the folded rotamer effect is also supported by calculations which arrive at an energy minimum for $\chi = 60°$ without the introduction of special interring forces,[38,39] although a simple van der Waals exclusion model could not predict the side-chain energy minimum.[40]

Conclusions

According to our interpretation of the CD and NMR data of the six N-methylated diketopiperazines studied, three have ring conformations in solution that differ significantly from the ring conformations found in their crystalline forms. The aliphatic compound c-(L-NMeVal)$_2$ and the aromatic derivatives c-(L-NMePhe)$_2$ and c-L-NMePhe-D-NMePhe maintain ring shapes close to those determined by X-ray analysis. The first is extremely sterically hindered; the second represents a case where the aromatic groups can interact with each other, with the diketopiperazine ring or with the solvent, depending on the nature of the rotamer; the third is an example of the tendency of aryl substituents to fold toward the diketopiperazine ring. The fact that some of these compounds exist in different states with opposing angles of ring fold implies that the N-methylated diketopiperazine ring may be considered somewhat flexible. This flexibility does not make the ring prone to protonation-induced shape changes. Strong proton-donating solvents TFA, H_2O, and chloroform/TFA have no apparent effect on the diketopiperazine ring structure.

Water does have a substantial effect on the distribution of aromatic side chain rotamers. Apparently, by folding both phenyl rings together over the diketopiperazine ring, c-(L-NMePhe)$_2$ achieves the minimum nonpolar surface exposure and therefore minimum solvent disruption. In less polar media, where the phenyl rings may solvate easily, there is a negligible problem with solvent disruption.

Acknowledgments. During the experimental phase of this research, W.R. was supported by NIH Postdoctoral Fellowship 1 F22 HD01942. Preparation of the manuscript was accomplished with support from the Cerebrovascular Gift Account of the Department of Neurological Surgery, College of Physicians and Surgeons, Columbia University, a fund whose contributions are from grateful patients. We wish also to acknowledge the support of this work by the NIH under Grant No. GM 18694. We want to thank Professor Sherman Beychok of Columbia University, in whose laboratories a few final experiments were carried out. The authors gratefully acknowledge the assistance of Dr. Grant Willson and Mr. Fred Vernacchia for the preparation of several of the key compounds. We want especially to acknowledge Mr. Wayne Becktel for his critical comments and helpful interpretations.

(39) Caillet, J.; Pullman, B.; Maigret, B. *Biopolymers* **1971**, *10*, 221.
(40) Growne, G.; Kenner, G. W.; Rogers, N. H.; Sheppard, R. C.; Titlestad, K. In "Peptides, 1968"; Bricas, E., Ed.; North-Holland Publishing Co.: Amsterdam, 1968; p 28.

Infrared Matrix-Isolation Studies of the Interactions and Reactions of Group 3A Metal Atoms with Water

R. H. Hauge,* J. W. Kauffman, and J. L. Margrave*

Contribution from the Chemistry Department, Rice University, Houston, Texas 77001.
Received January 7, 1980

Abstract: It has been shown that aluminum atoms react spontaneously with H_2O at 15 K while the heavier group 3A metals form M···OH_2 and M_2···OH_2 adducts. Adduct formation causes the ν_2-bending mode of H_2O to decrease by 21.4, 16.5, and 9.6 cm^{-1} for Ga, In, and Tl and 14.4 and 10.6 cm^{-1} for Ga_2 and In_2, respectively. The divalent HAlOH molecular species is formed from reaction of the aluminum atom with water. The HGaOH and HInOH molecular species are formed by photolysis of the respective adducts while the Tl···OH_2 adduct does not react on photolysis. The monovalent molecular species MOH is readily formed by further photolysis of the divalent HMOH species. Molecular vibrational frequencies and mode assignments are given in accompanying tables. Data suggest that the diatomic Ga_2, In_2 and Tl_2 adducts with water readily rearrange when photolyzed to a hydrogen-bridged dimetal species, which in turn is converted to the M_2O molecular species by further photolysis.

I. Introduction

Our understanding of molecular beam–water reactions,[1] water-induced thin film impurities, and surface–water reactions of the group 3A metals depends in part on our knowledge of the reactivity and reaction paths of atomic and small metal clusters of the group 3A metals with water. The matrix-isolation technique along with in situ photolysis affords the opportunity of following the reaction of an atom, diatom, etc., with water from initial interaction, through intermediate products to the final products.

Previous experimental[2,3] and theoretical[4] studies have shown that matrix-isolated alkali metals will form metal–water adducts.

(1) S. B. Oblath and J. L. Gole, *J. Chem. Phys.*, **70**, 581 (1979).
(2) R. H. Hauge, P. F. Meier, and J. L. Margrave, *Ber. Bunsenges. Phys. Chem.*, **82**, 102 (1978).
(3) P. F. Meier, R. H. Hauge, and J. L. Margrave, *J. Am. Chem. Soc.*, **100**, 2108 (1978).
(4) M. Trenary, H. F. Schaefer III, and P. A. Kollman, *J. Chem. Phys.*, **68**, 4047 (1978); *J. Am. Chem. Soc.*, **99**, 3885 (1977).

0002-7863/80/1502-6005$01.00/0

Table I. Estimated Heats of Reaction[a] (kcal/mol) for M + H_2O to Yield Various Products

			H + MOH		
M	HMOH	H_2 + MO	IIIA	IA	M
B	−81	−64	−28[b]	+15	Li
Al	−56	−6	−10	+40	Na
Ga	−21		+18	+35	K
In	−2		+34	+39	Rb
Tl	+9		+50	+31	Cs

[a] Estimated and measured M–OH bond energies were taken from ref 5. Estimated M–H bond energies were taken as equal to the respective group 2A hydride values found in ref 6. [b] BOH may also rearrange to HBO with an estimated ΔH of −10 kcal/mol.

It was also observed that photolysis caused further reaction to occur. The photolysis products of a lithium–water adduct were, as might be expected, lithium hydroxide and a hydrogen atom. Theoretical calculations[4] have indicated that lithium and sodium atoms bond to water through the oxygen with strengths of 11.7 and 5.2 kcal/mol, respectively, which may be compared to the observed ν_2 bending mode decreases of 17.5 and 7.4 cm^{-1} for water when bonded to lithium and sodium.[2] This comparison suggested that metal atom–water bond strengths may parallel measurable changes in the ν_2 bending mode of H_2O, and further evidence will be considered here.

A number of interesting products can form in group 3A metal–water reactions. From Table I, where estimated heats of reaction are shown, one sees that reactions of the alkali metals are endothermic as compared to aluminum, which has three exothermic or thermally neutral reaction paths, and gallium and indium, which have one exothermic path each. Thus, aluminum, gallium, and indium atoms are likely to react spontaneously with water. Experiments where the various group 3A metals are cocondensed with water in excess argon provide an opportunity to investigate whether spontaneous reaction does, in fact, occur and in any case allows one to study the nature of intermediate reaction products.

II. Experimental Section

Matrix experiments were carried out with an Air Products Displex closed cycle refrigerator, Model CSW-202. Matrices were formed on one of four polished surfaces of a copper block in good thermal contact with the second stage of the refrigerator. Argon was used in all studies and was brought in through 0.125-in. tubing positioned above and below and 1 in. from the trapping surface. A thermocouple gauge located 4 in. upstream was used to monitor the argon deposition rate. Input rates in the range of 1.5 mm/h, corresponding to a thermocouple reading of ~150 μ, were used. Water was brought in through a side port with 0.125-in. tubing. A thermocouple gauge which gave relative measures of water input rates was located ~24 in. upstream through 0.125-in. tubing from the vacuum exit. Typical gauge readings varied from 50 to 300 μ. The lowest setting gives 20% absorption for the strongest 1624.0-cm^{-1} peak of H_2O after a 1-h trapping. Relative ratios of argon to water or metal atoms were not measured, but argon was in appreciable excess. The rates of metal deposition were judged by both the temperature of vaporization and the rate of coloring evident as the matrix formed.

Matrices were irradiated either during or subsequent to the trapping process. The lamp used was a 100-W short-arc mercury lamp and was focused to a 0.75-in. diameter spot on the matrix surface. A water–Pyrex filter with various Corning long-pass cutoff filters was used for wavelength-dependent photolysis studies.

The respective metals were vaporized from containers heated by a surrounding 1-mil 0.375-in. tantalum foil heating element 3 in. long which was spot welded to 20-mil tantalum 0.250 in. wide straps. Gallium, indium, and thallium were vaporized from alumina containers over temperature ranges of 800–1100, 850–1000, and 550–700 °C, respectively. Aluminum was vaporized from a molybdenum container over a temperature range from 1075 to 1280 °C. Difficulties were encountered due to the wetting ability of aluminum which allowed it to creep out of the container and react with the tantalum heater; however, the rate of reaction was such that a series of matrices at different aluminum trapping rates could be formed without loss of the heating element. Isotopic forms of water have been used as reactants to help establish reaction product identity. $H_2{}^{18}O$ (95%) was obtained from Prochem Isotopes. The dependence of relative peak intensities on deposition rates also helps in this identification process.

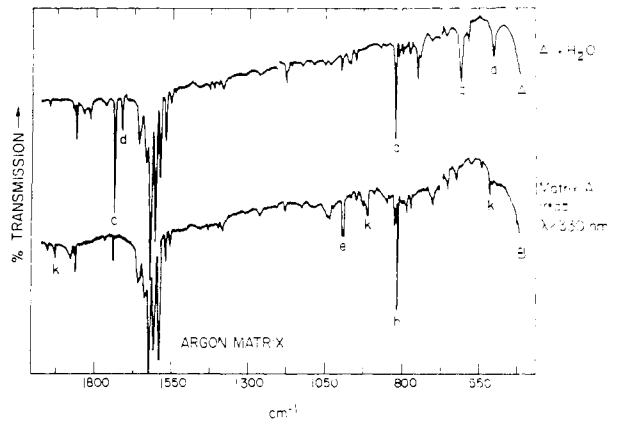

Figure 1. Infrared argon matrix spectra of products from the reaction of aluminum atoms with water (cm^{-1}). (A) Al + H_2O. (B) Matrix A was irradiated through a Pyrex–water filter with a focused 100-W short arc mercury lamp for 5 min.

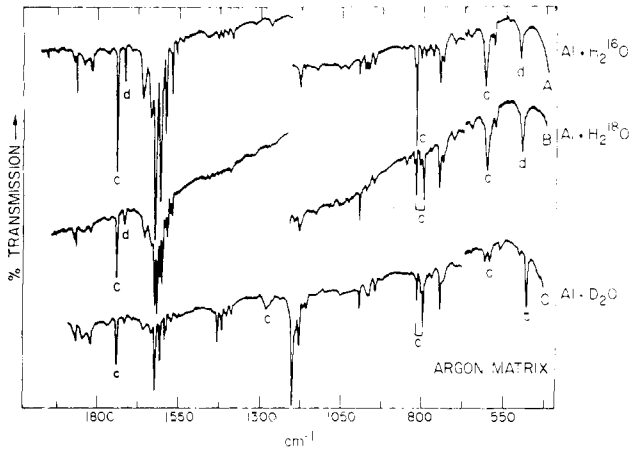

Figure 2. Infrared argon matrix spectra of products from the reaction of aluminum atoms with H_2O, $H_2{}^{18}O$, and D_2O (cm^{-1}): (A) Al + $H_2{}^{16}O$; (B) Al + $H_2{}^{18}O$; (C) Al + D_2O.

III. Results

A. Aluminum and Water. Cocondensation of aluminum with water in excess argon at 15 K gives a greenish-colored matrix. Infrared spectra taken immediately after deposition are shown in Figure 1A. Peaks labeled "c" and "d" can be assigned to reaction products of aluminum and water. Other peaks near 1875 and 745 cm^{-1} remain unassigned. However, water concentration studies indicate that they are not the result of aluminum–water reactions.

The area near the ν_2 bending mode of H_2O was carefully examined for any new features indicative of the Al···OH_2 adduct but without success. Thus, it appears that aluminum atoms react spontaneously with H_2O at 15 K. Variation of the water deposition rate indicates that the "d" peaks are favored by the highest water deposition rates and suggests that more than one H_2O molecule is involved in their production. Figures 2B,C illustrate the effects of oxygen-18 and deuterium isotopic substitution. It is clear that the 818-cm^{-1} "c" peak represents a metal–oxygen stretching mode. A slight decrease in the 605-cm^{-1} peak is also observed with oxygen-18 substitution.

The effect of deuterium substitution is less obvious for the 1743-cm^{-1} peak, but a broad, weak peak at 1280.9 cm^{-1} in Figure 2C is assigned as the deuterium counterpart. The apparent weakness is thought to be due to mixing with a combination of two lower modes. This point will be discussed in more detail later. The deuterium shift of the 818-cm^{-1} peak indicates that this mode is an Al–OH stretching mode. The other two peaks undergo large

Table II. Measured Vibrational Frequencies of HMOH and HMOH(H_2O) Species Isolated in an Argon Matrix (cm^{-1})

"c"	H-O stretch	M-H stretch	HMO bending	M-OH stretch	MOH bending
HAlOH	3743	1743.3	605.4	817.9	
$HAl^{18}OH$		1743.1	602.8	793.9	
DAlOH		1280.9	473.6	797.2	
$H^{69}GaOH$	3675	1669.8	784.9	646.4	520.5
$H^{71}GaOH$	3675	1669.8	784.9	644.7	520.5
$H^{69}Ga^{18}OH$	3660	1669.4	782.4	617.4	520.3
$H^{71}Ga^{18}OH$		1669.4	782.4	615.8	520.3
$D^{69}GaOD$	2708	1213.8	582.9	644.6	
$D^{71}GaOD$	2708	1213.8	582.9	643.1	
HInOH	3663	1486.3*[a]	713.4	548.0*[a]	
$HIn^{18}OH$		1486.5*[a]	711.0	520.9*[a]	
DInOD		1080.1*[a]		550.9*[a]	
"d"		**M-O stretch**	**HMO bending**	**M-OH stretch**	
$HAlOH(H_2O)$		1718.0	497.8	756.7	
$HAl^{18}OH(H_2{}^{18}O)$		1718.0	496.4	733.2	
$HGaOH(H_2O)$			728.6		
$HGa^{18}OH(H_2{}^{18}O)$			727.1		
$DGaOD(D_2O)$			532.2		

[a] These peaks have lower frequency shoulders.

Table III. Measured Vibrational Frequencies of MOH Group 3A and $HAl(OH)_2$ Species Isolated in an Argon Matrix (cm^{-1})

h	O-H stretch	M-OH stretch	MOH bending	M-OH (calcd)	(M-OH) $\Delta\nu$
AlOH	3790	810.3		810.3	
$Al^{18}OH$		785.2		784.2	−1.0
AlOD		795.2		796.7	1.5
$^{69}GaOH$	3692	613.0	424.4	613.0	
$^{71}GaOH$	3692	611.4	424.4		
$^{69}Ga^{18}OH$		588.4	421.9	586.5	−1.9
$^{71}Ga^{18}OH$		586.8	421.9		
$^{69}GaOD$	2721	595.8		599.2	3.4
$^{71}GaOD$	2721	594.4			
InOH		522.8	421.8	522.8	
$In^{18}OH$		502.4	419.0	498.2	−4.2
InOD		505.7		510.0	5.0
TlOH[a]		447.9			

K	M-H stretch	M-OH stretch	HMO bending
$HAl(OH)_2$	1934.9	910.6	511.4
$HAl(^{16}OH)(^{18}OH)$	1934.9	900.2	
$HAl(^{18}OH)_2$	1934.7	889.0	510.7
		unassigned	
$In(H_2{}^{16}O)$[b]		472.1	
$In(H_2{}^{18}O)$		450.9	
$In(D_2O)$		461.8	

[a] Species assignment tentative. The other possibility is TlOH-(H_2O). [b] Possible assignment is $InOH(H_2O)$.

frequency shifts with deuterium substitution and must be due primarily to hydrogen modes. Thus, the 1743-cm^{-1} peak is assigned to an Al–H stretching mode and the 605-cm^{-1} peak to one of the two possible in-plane hydrogen bending modes for the insertion product HAlOH. The measured values of respective "c" peaks and their isotopic counterparts are given in Table II. The "d" peaks are also listed in Table II and are tentatively assigned to a monohydrated HAlOH product.

Photolysis causes disappearance of both the "c" and "d" peaks as shown in Figure 1B and the growth of "h", "e", and "k" peaks. The "e" peak can be assigned to the Al_2O species as it appears at the same frequency and has the same oxygen-18 dependence as that observed in matrix-isolation studies of Al_2O.[7] The "h" peaks are observed at low water concentrations and clearly result from photolysis of the HAlOH insertion product. The loss of a peak in the Al–H stretching region suggests that the Al–H bond is broken during photolysis producing the species AlOH. The oxygen-18 and deuterium shifts of the "h" peaks are in agreement with its assignment to AlOH. The measured peak positions are given in Table III.

The "k" peaks are most intense after photolysis when strong "d" peaks were present prior to photolysis. A mixed $H_2{}^{16}O$–$H_2{}^{18}O$ reaction with aluminum at high water concentrations produces an equally spaced triplet at the 905-cm^{-1} "k" peak position which indicates the presence of two equivalent oxygens. The 1935-cm^{-1} peak indicates the presence of an Al–H bond. The most likely

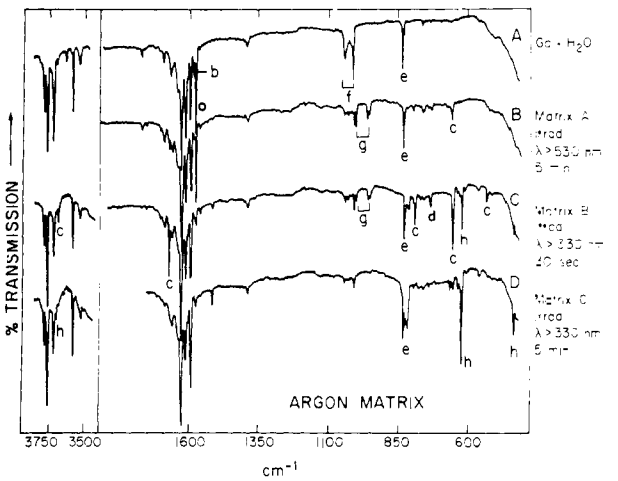

Figure 3. Infrared argon matrix spectra of products from the reaction of gallium atoms with water: (A) gallium (935 °C) and H_2O (100 μ); (B) the matrix was irradiated for 5 min through a Corning filter 3-68 (λ >530 nm); (C) the matrix was irradiated for 30 s through a Pyrex–water filter; (D) same conditions as (C) but with an additional 5 min of irradiation.

Table IV. Measured Frequencies for the Water (ν_2) Bending Mode in Group 3A–Water Adducts Isolated in an Argon Matrix (cm^{-1})

	H_2O		$H_2{}^{18}O$		HDO		D_2O	
M	$\tilde{\nu}$	$\Delta\tilde{\nu}$	$\tilde{\nu}$	$\Delta\tilde{\nu}$	$\tilde{\nu}$	$\Delta\tilde{\nu}$	$\tilde{\nu}$	$\Delta\tilde{\nu}$
	1593.3		1586.9		1402.6		1176.7	
Ga (a)	1571.9	21.4	1565.6	21.3	1384.9	17.7	1163.6	13.1
Ga_2 (b)	1578.9	14.4	1572.4	14.5	1390.7	11.9	1167.7	9.0
In (a)	1576.8	16.5	1570.4	16.5	1388.7	13.9	1166.4	10.3
In_2 (b)	1582.7	10.6					1170.0	6.7
Tl (a)	1585.3	8.0						
	1583.5	9.8						

(5) D. D. Jackson, "Thermodynamics of the Gaseous Hydroxides", UCRL-51137, Lawrence Livermore Laboratory, Livermore, Calif. 94500.
(6) A. G. Gaydon, "Dissociation Energies and Spectra of Diatomic Molecules", Chapman and Hall, London, 1968.
(7) D. M. Makowiecki, D. A. Lynch, Jr., and K. D. Carlson, *J. Phys. Chem.*, **75**, 1963 (1971).

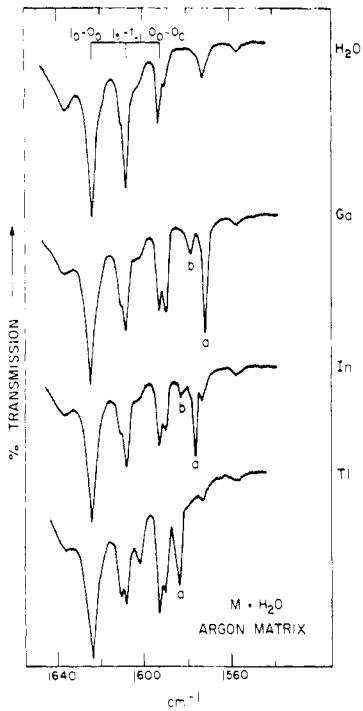

Figure 4. Infrared argon matrix spectra of the water bending mode region where water was cocondensed with Ga, In, and Tl. Trapping time was 1 h. The vaporization temperatures of Ga, In, and Tl were 950, 920, and 710 °C, respectively.

Table V. Measured Vibrational Frequencies of HM_2OH Group 3A Species Isolated in an Argon Matrix (cm^{-1})

	f		g			
HGa_2OH	1030	1002.1		994.9	950.5	945.6
$HGa_2{}^{18}OH$	1030	1002.1		993.6	949.8	945.5
DGa_2OD		741.6		722.1	678.6	
HIn_2OH			1045.2	919.9	915.6	912.0
$HIn_2{}^{18}OH$			1042.2		912.9	
DIn_2OD			804.7	681.0	675.5	672.6
HTl_2OH	928			874.3	859.0	

species assignment appears to be $HAl(OH)_2$, which could readily form from the assigned "d" species $HAlOH(H_2O)$. The measured peak positions are also given in Table III.

B. Gallium and Water. Cocondensation of gallium with water in excess argon at 15 K gives a bluish-green colored matrix. Infrared spectra taken immediately after deposition are shown in Figure 3A. The ν_2 bending mode region of H_2O is shown in more detail in Figure 4. The two peaks labeled "a" and "b" are assigned to a gallium–water adduct and listed in Table IV. The "b" peak increased relative to the "a" peak at high gallium deposition rates and is assigned to the $Ga_2{\cdots}OH_2$ adduct. The "f" peaks apparently result from reaction of gallium with water during the trapping process. The reactive species is thought to be Ga_2 for reasons discussed later. The "e" peak is due to Ga_2O from a small amount of gallium oxide present in the gallium.[7]

The "g" peaks grow in after elimination of the "b" and "f" peaks by photolysis with a long-pass cutoff filter ($\lambda > 580$ nm). This would indicate that the "g" peaks are due to a digallium species since the "a" peak is not affected. Both the "f" and "g" peaks are listed in Table V. Brief irradiation with shorter wavelength light causes an elimination of the "a" peak and a growth in "c" peaks as shown in Figure 3C. Thus, the "c" peaks are assigned to a monogallium species and listed in Table II. Prolonged irradiation causes the "h" peaks and new peaks near the "e" peak to grow. The new "e" peaks can also be assigned to Ga_2O from previous studies[7] and represent slightly different matrix sites for Ga_2O. The "h" peaks appear to result from photolysis of the "c" species. Their measured values are given in Table III.

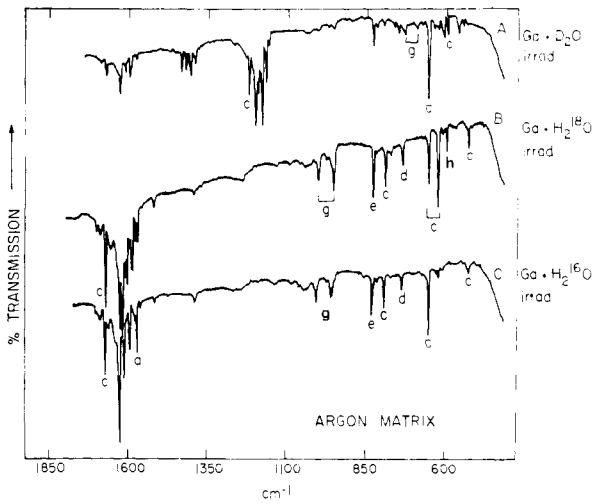

Figure 5. Infrared argon matrix spectra of products from the reaction of gallium atoms with water. Each matrix was irradiated for 10 s through a Pyrex–water filter ($\lambda > 330$ nm): (A) Ga and D_2O; (B) Ga and $H_2{}^{18}O$; (C) Ga and $H_2{}^{16}O$.

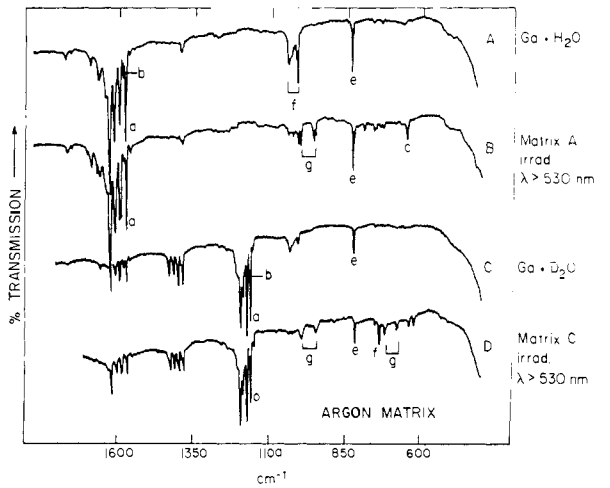

Figure 6. Infrared argon matrix spectra of products from the reaction of gallium atoms with water: (A) gallium (935 °C) and H_2O (100 μ); (B) matrix from (A) was irradiated for 5 min with Hg short arc lamp and a Corning 3-68 ($\lambda > 530$ nm) filter; (C) gallium (1080 °C) and D_2O (150 μ); (D) matrix (C) irradiated with same conditions as (B).

Isotopic shift data, as illustrated in Figure 5 and given in Tables II and III, confirm the presence of a single gallium and oxygen atom in species "c" and "h". The gallium isotopic peaks possess the same relative intensities as expected from the abundance of the ^{69}Ga (60.4%) and ^{71}Ga (39.6%) isotopes. Peaks "f" and "g" undergo a large deuterium shift as illustrated in Figure 6 and given in Table V, but almost no oxygen-18 shift. Thus, they can be assigned to hydrogen vibrational modes. Their close proximity suggests that they may be due to similar species. A hydrogen mode at ~ 1000 cm^{-1} is surprising in that it is much lower than the terminal H–Ga frequency at 1670 cm^{-1} for the "c" species and considerably higher than that expected for a hydrogen bending mode. It is reasonable to expect an asymmetric bridging hydrogen mode in this wavenumber region; thus, the "g" and "f" species may represent the case where water has reacted with Ga_2 to give a bridging hydrogen and a bridging hydroxyl group. The corresponding mode for the hydroxyl group is expected to occur below 400 cm^{-1}. This species apparently loses both hydrogens and is converted to Ga_2O by prolonged photolysis at shorter wavelengths.

It is evident from the above data that gallium atoms, unlike aluminum atoms, form a stable adduct with water. The presence of the "f" species with a bridging hydrogen mode immediately after trapping indicates that a diatomic gallium is partially reacting during the trapping period. However, the presence of the "b" adduct indicates that some diatomic gallium–water adduct is

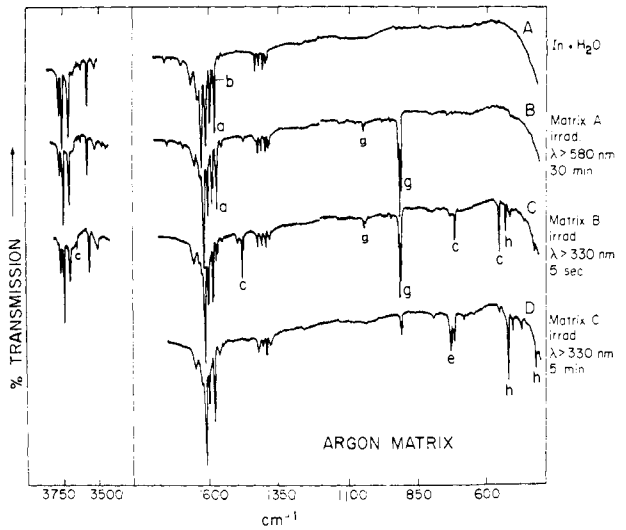

Figure 7. Infrared argon matrix spectra of products from the reaction of indium atoms with water: (A) In (920 °C) and H_2O (105 μ); (B) 30-min irradiation of (A) through Corning filter no. 2-73 ($\lambda > 580$ nm); (C) 5-s irradiation of (B) through a Pyrex–water filter ($\lambda > 330$ nm); (D) 5-min irradiation of (C) ($\lambda > 330$ nm).

formed. The slightly different values of the "f" and "g" peaks could easily result from closely related structural isomers and different matrix sites.

The "c" species can be best explained as the HGaOH insertion product. The "h" species results from loss of the H–Ga bond in HGaOH and is thus assigned to GaOH. Weak peaks of 1514 and 1090 cm^{-1} for H_2O and D_2O reactions, respectively, are also observed when the "h" peaks are produced. The vibrational frequency of GaH in the gas phase is 1546.9 cm^{-1}, which suggests that the above peaks are due to formation of GaH and GaD as would be expected from reaction with a nearby gallium atom of the hydrogen atom produced in the photolysis of HGaOH.

C. Indium and Water. Cocondensation of indium with water in excess argon gives a green-colored matrix. Infrared spectra taken immediately after deposition are shown in Figure 7A. The ν_2 bending mode region of H_2O is shown in more detail in Figure 4. The peaks labeled "a" and "b" are assigned to an indium–water adduct and listed in Table IV. The "b" peak increases relative to the "a" peak at high indium deposition rates and is assigned to the $In_2 \cdots OH_2$ adduct. Irradiation with a long-pass cutoff filter, $\lambda > 580$ nm, causes a loss of the "b" peak and growth of the "g" peaks as shown in Figure 7B, which indicates that the "g" peaks are due to a diindium species. The "g" peaks are listed in Table V. Brief irradiation with shorter wavelength light eliminates the "a" peak and gives the new peaks labeled "c" and "h". Further irradiation with the same light removes the "g" and "c" peaks and causes a growth in the "e" and "h" peaks. The "e" peaks can be assigned to the In_2O species[7] and most likely result from further photolysis of the "g" species. The "h" species grows as a result of photolysis of the intermediate "c" species. The "c" and "h" peaks are given in Tables II and III, respectively.

The effect of oxygen-18 and deuterium isotopic substitution is shown in Figures 8 and 9. The "g" peaks are affected only slightly by oxygen-18 substitution but undergo a large shift with deuterium substitution as would be expected for a mode due primarily to hydrogen. The wavenumber value of the "g" peaks suggests that they be assigned to a bridging hydrogen in the HIn_2OH species. This would require the presence of a bridging hydroxyl; however, its vibrational modes are expected to fall below 400 cm^{-1}.

The species "c" and "h" are seen to contain only one oxygen from mixed $H_2{}^{16,18}O$ reactions. They also contain only one indium atom since they result from photolysis of the "a", $In{\cdot}OH_2$, adduct species. The 1485-cm^{-1} "c" peak can be assigned to a terminal H–In bond. The 547-cm^{-1} "c" peak undergoes an oxygen-18 and deuterium shift which is best explained by assigning it to an In–OH stretching mode. The other labeled "c" peak is a hydrogen mode

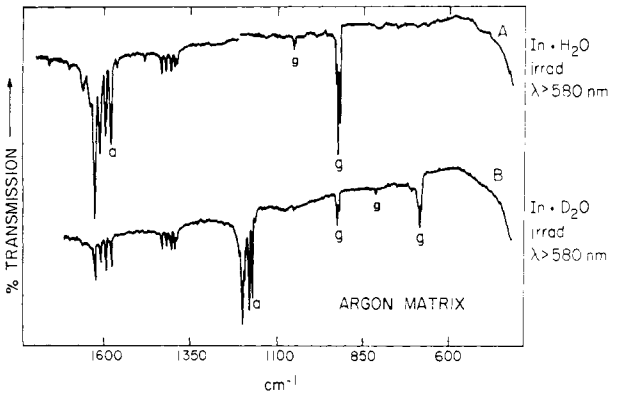

Figure 8. Infrared argon matrix spectra of products from the reaction of indium atoms with water: (A) indium (920 °C) and H_2O (105 μ) after irradiation for 30 min through Corning filter 2-73 ($\lambda > 580$ nm); (B) indium (983 °C) and D_2O (150 μ) with irradiation during trapping ($\lambda > 580$ nm).

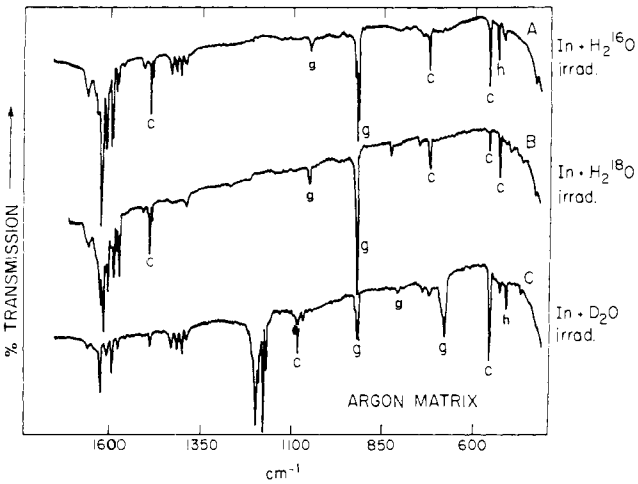

Figure 9. Infrared argon matrix spectra of products from the reaction of indium atoms with water: (A) In (920 °C) and H_2O (105 μ); (B) In (925 °C) and $H_2{}^{18}O$ (150 μ); (C) In (983 °C) and D_2O (150 μ). In each case the matrix was irradiated through a Pyrex–water filter after trapping.

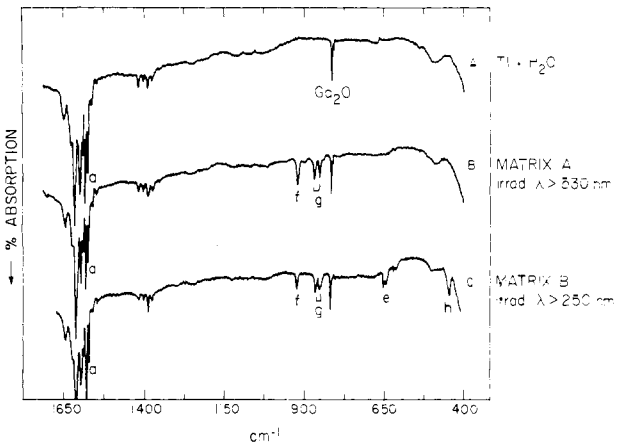

Figure 10. Infrared argon matrix spectra of products from the reaction of thallium with water: (A) thallium (710 °C) and H_2O (145 μ) after 1 h deposition; (B) matrix (A) was irradiated through a Corning filter 3-68 ($\lambda > 530$ nm) for 35 min; (C) matrix (B) was irradiated for 15 min with full light of mercury short arc lamp.

and is thought to be due to the bending mode of the terminal hydrogen. The "c" species is thus assigned as the insertion product HInOH.

The "h" species results from photolysis of the HInOH with elimination of the two highest modes previously identified with the H–In bond. Thus, the "h" species is assigned as InOH.

D. Thallium and Water. Cocondensation of thallium with water in excess argon gives a blue-colored matrix. Infrared spectra taken immediately after deposition are shown in Figure 10. The ν_2 bending mode region of H_2O is shown in more detail in Figure 4. Only one closely spaced doublet peak labeled "a" could be seen, and it is listed in Table IV. The expected "b" peak is most likely hidden by the water peaks. Irradiation with a long-pass cutoff filter ($\lambda > 530$ nm) gives the "f" and "g" peaks as shown in Figure 10B and listed in Table V. No loss in either doublet of the "a" peak intensity was observed and it is thought that the "f" and "g" species are coming from photolysis of a $Tl_2\cdots OH_2$ adduct species whose "b" peak is hidden. Further irradiation with shorter wavelength light reduces the intensity of both the "f" and "g" peaks and eliminates the higher doublet of the "a" peak while producing the "e" and "h" peaks. The "h" peak is given in Table III. The "e" peaks can be assigned to Tl_2O.[7] Thallium behaves differently than gallium and indium since the major "a" peak which is assigned to the $Tl\text{–}OH_2$ adduct species is not appreciably changed by prolonged photolysis. This point will be discussed later. The "f" and "g" peaks, where the distinction between "f" and "g" is due to their photolytic behavior which was similar to that of gallium, are tentatively assigned to a hydrogen bridging HTl_2OH species. The assignment of the "h" peak is uncertain, but a suggested assignment is that of TlOH or $TlOH(H_2O)$. The hydrated species could result from a $Tl\cdots(H_2O)_2$ adduct which in turn is responsible for the higher frequency doublet of the "a" peak.

Discussion

Calculations and experiments[2-4,8] suggest that when water bonds to Li, Na, and Al through the oxygen an adduct of C_{2v} symmetry is formed. Calculations have also shown that the metal becomes slightly negative in the adduct owing to a small amount of electron donation from water to the metal as might be expected in a Lewis acid–base type interaction. The sensitivity of the ν_2 bending mode of water to adduct formation may be understood by reference to the photoionization spectra of water[9] which indicate that ionization from the $1b_1$ orbital causes small decreases in both the bending ($\Delta\nu = -225$ cm^{-1}) and stretching ($\Delta\nu = -437$ cm^{-1}) frequency of water along with a bond-angle increase of $\sim 5°$. Ionization from the $2a_1$ orbital results in a large decrease in the bending mode ($\Delta\nu = -687$ cm^{-1}) and no observable change in the stretching mode, as well as a bond-angle increase to 180°. The ν_2 bending mode and bond angle of water are clearly much more sensitive to electron loss from the $2a_1$ (σ lone pair) orbital of water than the $1b_1$ (π lone pair) orbital. As mentioned by Potts and Price,[9] the $2a_1$ orbital in a linear AH_2 molecule is nonbonding and in a bent molecule acts primarily as a shield to the mutual repulsion of the two hydrogen nuclei. Thus, one expects electron density loss in the region between the hydrogens to lead to a larger angle and lower frequency. Little effect would be expected on the oxygen–hydroxy bonds because of the largely nonbonding character of the $2a_1$ orbital with respect to these bonds. Consequently, electron donation from the $2a_1$ orbital of water into the partially or unoccupied a_1 orbitals of the metal should be marked by a decrease of the bending mode frequency but little or no change in the stretching modes.

The $1b_1$ orbital is also nonbonding in a linear AH_2 molecule but does not provide significant stabilization of the bent molecules as does the $2a_1$ orbital. As a result, electron donation from the water $1b_1$ orbital into a b_1 orbital of the metal should not affect the bending frequency of water.

Thus changes in ν_2 should primarily reflect perturbation or σ bonding to the metal of the $2a_1$ orbital of water. Our general observations indicate a decrease in the bending mode of water and no observable shift in the stretching modes of water upon formation of a metal–water adduct.

A comparison of the shifts in the ν_2-water bending mode for water adducts of the alkali metals Na (−7.4 cm^{-1}), K (−6.6 cm^{-1}), and Cs (−2.7 cm^{-1}) to the group 3A metal of the same row indicates a factor of 3 increase in $\Delta\nu_2$ for the group 3A metals. This suggests that the corresponding group 3A metal interacts much more strongly with a water molecule than the respective alkali metal atom. Since aluminum reacted spontaneously, a measured $\Delta\bar{\nu}$ was not obtained but one can estimate a value of −24 cm^{-1} by comparison to $Na\cdots OH_2$. Assuming a general linear relationship between $\Delta\bar{\nu}$ and interaction energy, one predicts an interaction energy of ~ 16 kcal for $Al\cdots OH_2$ by comparison to Li (17.5 cm^{-1}, 11.7 kcal).[4] This may be compared to values of 4.4 and 8.5 kcal from calculations of Trenary[4] and Kurtz,[8] respectively. The lack of agreement between the calculated and estimated value suggests that the correlation between $\Delta\bar{\nu}$ and interaction energy is not a general one and that it may work only within a specific group. This is not surprising if the bending frequency is reflecting only σ donation of the water and not π bonding of the $1b_1$ orbital or back-bonding from the metal into the unoccupied $2b_2$ antibonding orbital of water.

Although the quantitative relationship of $\Delta\bar{\nu}$ to interaction energies is unclear, it seems likely that the interaction energies should follow in some manner the $\Delta\bar{\nu}_2$ change. Thus it appears that the diatomic group 3A molecules are more weakly bonded to water than is the atom. One expects Ga, In, and Tl atoms to bond in a similar manner to aluminum atoms;[4,8] however, the type of interaction between diatomic species and water is not obvious since it may either exist as an interaction with a single metal atom or as a bridging interaction with both atoms.

The photoinduced reactivity of the group 3A metal–water adduct with respect to formation of the divalent metal hydroxyhydride is seen to vary from spontaneous reaction for aluminum to no reaction for thallium. It is interesting that the inability to form HTlOH agrees with the ΔH estimate given in Table I which indicates that HTlOH is unstable with respect to $Tl\cdots OH_2$.

The HMOH molecule is expected to have C_s symmetry owing to the presence of the one unpaired electron which should result in an HMO bond angle of less than 180°. The number of infrared-active modes would be six with the two lowest modes being MOH bond angle deformations both in and out of the molecular plane. The trend of assigned HMO bending mode with respect to atomic number exhibits unusual behavior in that the aluminum HAlO bending mode is less than that for gallium and indium. This may be due to a decreased HMO bond angle for the heavier group 3A atoms as is the case for the group 4A metal dihalides.

This behavior is also evident in the assigned MOH bending mode for HGaOH. A similar mode was not observed for HAlOH under conditions where the other modes of HAlOH were quite strong. Thus it seems likely that its value is less than that for gallium and less than 400 cm^{-1}.

It was mentioned earlier that the deuterium stretching mode of DAlOD was much weaker and broader than expected. This is thought to result from a Fermi interaction of the D–Al stretching mode with a combination of the DAlO bending and Al–OD stretching modes.

The isotopic shifts, in general, confirm the assignment of observed frequencies to particular modes. However, one notes that the M–OH mode undergoes rather strange shifts upon deuterium substitution. This is particularly evident for indium, where deuterium substitution causes an increase in the M–OH mode. This behavior can be explained if one assumes molecule C_s symmetry. With this molecular symmetry the three lowest observed modes are expected to undergo partial coupling to each other. Deuteration will cause changes in the extent of coupling between the modes which, in turn, leads to the unusual isotopic shifts. This coupling would not occur for a linear molecule with $C_{\infty v}$ symmetry. Thus its existence is further evidence for a nonlinear molecule.

A similar effect exists for the MOH molecules. This is evident from a comparison between calculated and measured isotopic shifts of the M–OH mode where the shifts have been calculated for a linear geometry and assumption of the absence of any coupling between the OH and M–OH stretching modes. The calculated shifts are compared to measured values in Table III. One sees

(8) H. A. Kurtz and K. D. Jordan, *J. Am. Chem. Soc.*, in press.
(9) A. W. Potts and W. C. Price, *Proc. R. Soc. London, Ser. A*, **326**, 181 (1972).

an increasing discrepancy between the calculated and measured values with increasing mass of the group 3A metal. These discrepancies can be explained by changed coupling of the MOH stretching and bending modes of a nonlinear molecule.

The photolytic reaction of diatomic group 3A molecules with water occurs at longer wavelengths than for the atom and produces a group of absorption peaks in the 850–1050-cm^{-1} region. Deuterium isotopic shifts indicate that the vibrational mode is primarily a hydrogen motion, although there is a slight oxygen-18 dependence. We have suggested that the mode may be best explained as an asymmetric mode of a bridging hydrogen. The location of modes due to a bridging hydrogen should be ~1000 and ~900 cm^{-1} for gallium and indium, respectively, if one assumes a similar ratio of frequencies as that found for the asymmetric bridging and terminal stretching modes of diborane. One also expects the hydroxyl group to be bridging. It is possible to view the HM_2OH molecule as a mixed dimer of monovalent MH and MOH species which suggests that dimers of MH and MOH would also exist as bridging structures. Prolonged photolysis at shorter wavelengths converts the HM_2OH species to the known high-temperature M_2O species.

The dihydroxyaluminum hydride has been identified and presumably results from further reaction of the $HAlOH(H_2O)$ species. We did not observe a similar dihydroxy species for gallium and indium, which may suggest that the higher oxidation state $HM(OH)_2$ is unstable with respect to the $MOH(H_2O)$ species. In fact, the unassigned peaks listed in Table III for indium could be due to $InOH(H_2O)$.

The inability of thallium to react was discussed earlier. However, after prolonged photolysis, we do observe a peak labeled "h". We have suggested that the peak may be assigned to TlOH or $TlOH(H_2O)$. Although the reaction is endothermic and the excited state HTl*OH is expected to revert to $Tl\cdots OH_2$, some probability may exist for breaking of the H–Tl bond and subsequent diffusion of the hydrogen into the matrix, thereby stabilizing the TlOH species. The alternative assignment as $TlOH(H_2O)$ formation could result from stabilization of TlOH by interaction with water. It is interesting to note that a dithallium product species does readily form, which suggests that a bridging structure has stabilized the hydrogen and hydroxyl bonds sufficiently to favor the photolysis product over the adduct.

The reaction chemistry of group 3A metals with water may be summarized as follows:

$$M + H_2O \rightarrow M\cdots OH_2 \xrightarrow{h\nu_1} HMOH \rightarrow H + MOH$$

$$M_2 + H_2O \rightarrow M_2\cdots OH_2 \xrightarrow{h\nu_2} \begin{matrix} & H & \\ M & & M \\ & O & \\ & H & \end{matrix} \xrightarrow{h\nu_1} M_2O + H_2$$

The exception is Al, which spontaneously reacts with water as follows:

$$Al + H_2O \rightarrow HAlOH \xrightarrow{h\nu_1} AlOH + H$$

$$Al + 2H_2O \rightarrow HAlOH(H_2O) \xrightarrow{h\nu_1} HAl(OH)_2 + H$$

Acknowledgments. Matrix-isolation spectroscopy and synthetic chemistry at Rice University are supported by funds from the National Science Foundation, the U.S. Army Research Office, Durham, and The Robert A. Welch Foundation.

A Nuclear Magnetic Resonance Study of *tert*-Butoxyaluminates

Deane A. Horne

Contribution from Bowman-Oddy Laboratories, Department of Chemistry, The University of Toledo, Toledo, Ohio 43606. *Received October 1, 1979*

Abstract: ^1H, ^7Li, ^{13}C, and ^{27}Al NMR studies of lithium *tert*-butoxyaluminates have been carried out in THF solution. While the ^7Li study was not particularly informative, the ^1H, ^{13}C, and ^{27}Al studies clearly show that $Li(t\text{-}BuO)AlH_3$ does not exist in THF solution in large enough concentration to be detected. It was found that the equilibrium $3Li(t\text{-}BuO)_2AlH_2 \rightleftarrows 2Li(t\text{-}BuO)_3AlH + LiAlH_4$ is present with $K_{eq} = 2.2 \times 10^{-2}$.

Introduction

Since the discovery of lithium aluminum hydride more than 30 years ago, considerable work has been devoted to modify its reactivity by the addition of alcohols to produce lithium alkoxyaluminum hydrides.[1] Because of the apparent stability of lithium *tert*-butoxyaluminum hydrides in tetrahydrofuran (THF) solution, and the selectivity of reduction by $Li(t\text{-}BuO)_3AlH$, *tert*-butyl alcohol has received the most attention as a modifying alcohol for $LiAlH_4$.[1b-d]

Two reports have appeared in the literature concerning the nature of the solute species for lithium *tert*-butoxyaluminum hydride. Kader[2] described a ^1H NMR study in ether–THF solvent in which he interpreted the proton resonances of his solutions as due to three species: $Li(t\text{-}BuO)AlH_3$, $Li(t\text{-}BuO)_2AlH_2$, and $Li(t\text{-}BuO)_3AlH$. Ashby[3] reported ebullioscopic and conductance measurements on THF solutions prepared by adding 1 or 3 mol of *tert*-butyl alcohol per mol of $LiAlH_4$. Ashby concluded that in THF $Li(t\text{-}BuO)_3AlH$ is monomeric over a concentration range of 0.05–0.5 m (association (i) ~ 1), and $Li(t\text{-}BuO)AlH_3$ is associated (i = 1.3 at 0.4 m). He did not report data for $Li(t\text{-}BuO)_2AlH_2$.

The new experiments described below involve ^1H, ^7Li, ^{13}C, and ^{27}Al NMR studies of 0.4 M solutions of $LiAlH_4$ in THF containing molar ratios of *tert*-butyl alcohol to $LiAlH_4$ of from 0.5 to 3.0. The results show that from molar ratio of 0.5 to 2.0 the predominant lithium *tert*-butoxyaluminate is $Li(t\text{-}BuO)_2AlH_2$. Evidence for $Li(t\text{-}BuO)AlH_3$ could not be found in THF even at molar ratios as low as 0.5.

Experimental Section

The $LiAlH_4$ solutions were prepared by stirring $LiAlH_4$ with anhydrous THF containing 1% v/w benzene-d_6 under nitrogen and filtering. The chemical shifts for ^{27}Al and ^7Li in $LiAlH_4$ were measured by sus-

(1) (a) For a review see: Malek, J.; Cerng, M. *Synthesis* **1972**, 217. (b) Brown, H. C.; McFarlin, R. F. *J. Am. Chem. Soc.* **1958**, *80*, 5372. (c) Haubenstock, H.; Eliel, E. *Ibid.* **1962**, *84*, 2363. (d) Brown, H. C.; Shoaf, C. J. *Ibid.* **1964**, *86*, 1079.

(2) Kader, M. *Tetrahedron Lett.* **1969**, 2301.

(3) Ashby, E. C.; Dobbs, F. R.; Hopkins, H. P., Jr. *J. Am. Chem. Soc.* **1975**, *97*, 3158.

0002-7863/80/1502-6011$01.00/0